Polyether Polyurethanes: Synthesis, Characterization, and Thermoresponsive Shape Memory Properties

J. Dyana Merline, C. P. Reghunadhan Nair, C. Gouri, G. G. Bandyopadhyay, K. N. Ninan

Propellants and Special Chemicals Group, Vikram Sarabhai Space Centre, Thiruvananthapuram 695022, India

Received 9 May 2007; accepted 26 September 2007
DOI 10.1002/app.27555
Published online 17 December 2007 in Wiley InterScience (www.interscience.wiley.com).

ABSTRACT: Thermoresponsive shape memory polymers based on polyurethane with soft segment consisting of poly (tetramethylene oxide) (PTMO) and hard segment arising from urethane reaction of tolylene diisocyanate with OH terminal of PTMO and 1,4 butane diol (BD) were synthesized by a two- step process. The molar ratios of the reactants were varied to get polymers of different soft – hard segment contents. These were characterized by DSC, IR, DMTA, XRD, SEM analyses, and mechanical properties. The shape memory behavior was evaluated by cyclic tensile tests. PTMO served as the switching segments whose crystalline melting was responsible for the switching behavior. As the hard segment-content increased, transition temperature (T_{trans}) diminished and so did the elongation and tensile strength of the polyurethane. Higher glassy/rubbery modulus ratio observed for higher hard segment-content polymer was conducive to better shape recovery properties. The influence of hard/soft segments on the thermal, mechanical, damping and shape memory properties of the copolymers are presented and correlated to their phase morphology, as investigated by FTIR and SEM. © 2007 Wiley Periodicals, Inc. J Appl Polym Sci 107: 4082–4092, 2008

Key words: shape memory polymer; polyurethane; phase separation; dynamic mechanical analysis; cyclic tensile test

INTRODUCTION

Thermoresponsive shape memory polymers (SMPs) are temperature-sensitive functional polymers, which find broad applications in temperature sensing elements. Excellent shape memory effects have often been observed with block or segmented copolymers.[1–6] SMPs have many advantages over shape memory alloys, like easy processing, low density, high recovery, high recoverable strain, and low manufacturing cost. Their recoverable strain is of the order of 100%, while shape memory metals and ceramics can recover only about 1–10%.[7,8] These polymers basically consist of two phases, a frozen phase (or fixed phase) and a reversible switching phase. The fixed phase could arise from the entanglement of polymeric chain or the chemical or physical cross-linked points and the reversible phase constituted by soft segments.[9–11] The processing and recovery of the SMP is schematically shown in Figure 1. When the polymer is deformed at a temperature above transition temperature (T_{trans}) and suddenly cooled to a temperature below T_{trans}, the deformed shape becomes frozen. When it is heated above T_{trans}, the polymer recovers its original shape.[12–16] SMP materials have the ability to recover large strains imposed by mechanical loading. They are designed to have a large change in elastic modulus above and below the transition temperature of the amorphous phase.[5] Characteristics such as shape recoverability and shape fixity exist because of the difference in mechanical properties of the material above and below the phase transition temperature.[17] Among the SMPs, polyurethanes have evinced increasing attention because of their excellent shape recovery characteristics as well as good elasticity and strength, depending on the nature and amounts of polyol, isocyanate and the chain extender.[18]

Polyurethane based SMPs have been reported in literature. While keeping the polyol as tetramethylene oxide (PTMO), a few diisocyanates have been used. Majority of the reported literature concerns shape memory PUs derived from 2,4-diphenyl methylene diisocyanate (MDI) and polycaprolactone.[1,4,5,7,9,11,13] Kim and coworkers studied the thermal, mechanical shape memory property of segmented thermoplastic PUs derived from polycaprolactone and MDI.[4,5,19] Lin and Chen studied the thermal, dynamic mechanical properties and the correlation of morphologies with shape memory effect of PUs based on PTMO and MDI.[9,11] A few reports concern use of tolylene diisocyanate (TDI) too.[20,21] These concern short reports on the demonstration of shape memory property of the derived PU. There have not been many systematic and quantitative studies on the effect of polymer molecular characteristics and the associated

Correspondence to: C. P. R. Nair (cprnair@gmail.com).

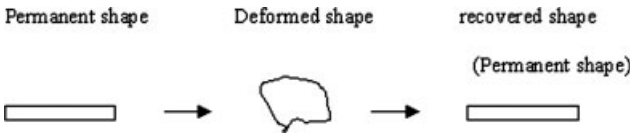

Figure 1 A Schematic representation of processing of SMP.

physicomechanical phenomenon on the shape memory characteristics of such systems. Present article deals with thermoplastic PU based on OH-terminated PTMO, TDI, and butane diol (BD) as chain extender and a quantitative aspect of their shape memory properties. The correlation of the shape memory property to the structure, composition and morphology of the polymer is examined.

EXPERIMENTAL

Materials

Hydroxy telechelic PTMO (Sigma-Aldrich, Hyderabad, India; M_n = 2000), BD (Alfa Biochem, India) and tolylene diisocyanate (TDI) (Aldrich) were used to synthesize PUs. PTMO and BD were dried in rotavapour for 3 h at 80°C before use. AR grade dimethyl formamide (DMF; SRL, India) was used as solvent.

Polymer synthesis

A 500 mL round bottomed, three neck flask equipped with a mechanical stirrer, a nitrogen inlet and a condenser with a drying tube was used for the synthesis of PUs. N_2 gas was bubbled at 40°C for 30 min through the dried PTMO in the flask to remove traces of absorbed moisture. To this, calculated amount of TDI was added drop-wise and the reaction mixture was stirred under N_2 at 65°C for 2 h to get the isocyanate terminated prepolymer. To this, a dilute solution of BD in DMF followed by the remaining quantity of TDI was added slowly at 65°C (total solid-content was kept at 30% in DMF). After mixing completely, the temperature was raised to 85°C and the reaction was continued for 3 h. The resultant polyurethane solution was poured on a glass plate and dried at 65°C/24 h followed by vacuum drying at 65°C/24 h to get a thin film. Samples for mechanical and cyclic tensile tests were cut from these films.

Polymer characterization

Physical, thermal and spectroscopic analysis

Thermal studies were performed in a Mettler DSC-20 analyzer. The samples (preserved in a dessicator) were heated from −50°C to 100°C at a heating rate of 5°C/min. DSC data of the first run was used for analysis. IR studies were done in Perkin Elmer GX-A model FTIR spectrophotometer. Spectra were recorded in the range of 4000 to 550 cm^{-1} with a resolution of 4 cm^{-1} using a thin film of the polymer. Inherent viscosity of 2% solution of the samples in DMF was determined at room temperature (25°C).

X-ray studies

X-ray scattering studies were performed in a 'X' Pertpro (P Analytical, Netherlands) using the filter Ni, the target as Cu Kα radiation (λ of 1.5405 Å) at 40 kV and 30 mA current. The diffraction patterns of the samples of thickness 1 mm were recorded with Bragg's angle 2θ from 0 to 40°. The crystallite size L_c of the samples were determined by using Scherrer equation,

$$L_c = K\lambda/\beta \cos\ \theta \quad (1)$$

where, λ = 1.5405 Å, K is the instrument constant taken as 0.89, β is the half value width in radians of the X-ray intensity vs. 2θ curve, and θ is the angle of reflection. The analysis was done at ambient temperature (25°C). In one case a sample kept at 0°C was subjected to XRD analysis, before it attained the room temperature. In this case, the analysis temperature is presumed to be 10–15°C.

SEM analysis

SEM analyses were performed in a Philips XL-30 instrument. Samples were gold coated in Denton vaccum apparatus. The samples were scanned at 150 kV with 500× magnification at ambient temperature.

Mechanical and cyclic tensile tests

Mechanical properties were determined with a tensile tester (UTM 4469) at ambient temperature (25°C). The micro tensile test specimens had the dimensions of 75 mm × 5 mm × 1 mm as per ASTM D 412. The gauge length and crosshead speed were 33 mm and 500 mm/min respectively. At least three specimens were tested, and the average was taken. Dynamic mechanical thermal analysis (DMTA) with samples of the same size as above was carried out between −100 and 250°C at a frequency of 1 Hz in DTemp Ramp type analyzer in the tensile mode. DMTA data of the second run was used for the analysis.

For carrying out cyclic tensile tests, the tensile specimens cut from the PU films of dimensions as above were used. The tests were done between the temperature T_g ± 20°C using a tensile tester (UTM Instron 1121) attached with a constant heating chamber. Loading and unloading, together with heating and cooling were done under controlled temperature

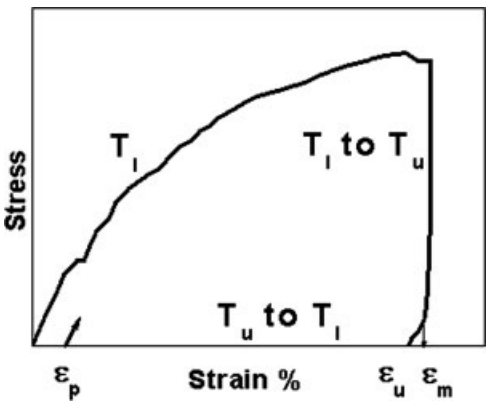

Figure 2 Schematic of a cyclic tensile test with loading at temperature above T_{trans}.

conditions. Figure 2 defines a thermomechanical cycling test with loading at high temperature T_1, (T_g + 20°C) adopted in our work. First, at the temperature T_1, the maximum strain ε_m (which was taken as the 50% strain of the strain at RT) is applied at a constant strain rate ε, and then maintaining ε_m, the temperature is cooled to T_u (T_g − 20°C). After holding at T_u for 5 minutes, it is unloaded. Upon removing the load at T_u, a marginal recovery of strain (ε_u) occurs. Under the no-load condition, it is heated from T_u to T_1 in 5 min and held for 5 min at T_1, allowing a recovery of strain (ε_r) where $\varepsilon_r = \varepsilon_m - \varepsilon_p$. This completes one thermomechanical cycle leaving a residual strain ε_p. Each system was subjected to five thermomechanical cycles. This methodology has been reported in many previous work.[4,17,19]

RESULTS AND DISCUSSIONS

Synthesis and characterization of PUs

Table I gives the formulations of PUs containing different soft/hard segment contents. A 1 : 1 stiochiometry of —OH and —NCO was employed in the study. The hard segment content consisting of TDI and BD was varied between 33 and 85 wt %. This calculation includes the urethane groups, associated aromatic ring and the chain extender.

Generally, the inherent viscosity decreased with increase in hard segment content as the polymer contains more of low molar mass TDI and BD units than the high molar mass PTMO units. Further increase in hard segment content would be expected to suppress the crystallization of PTMO because of the possibility of extensive intercalation of hard segment into PTMO phase by way of H-bonding. One way to offset this effect is to use higher molecular weight PTMO.

The transition temeperature (corresponding to maximum tan δ from DMTA) decreases with increase in hard segment content. This occurs because with increase in hard segment-content, the concentration of crystallisable PTMO segment decreases. The diminution in T_{trans} with hard segment –content also implies the possibility for the enhanced intercalation of hard segments into soft segment phase.[5] In this study, PTMO of molecular weight 2000 was used. It can be expected that if higher molecular weight PTMO is used, the increase in hard segment-content would practically not affect the crysatllisability and the crystalline transition temperature of the PTMO segments.

Differential scanning calorimetry

The DSC thermograms of various polymers in the dry state are shown in Figure 3. At higher PTMO concentration, its crystallization (at ≈ 28°C) and crystalline melting (at ≈ 73°C) are clearly seen. As the urethane-content increases, the melting point turn out to be more diffuse and the thermal profile corresponding to the ''melting'' resembles a ''glass transition-like'' at temperatures are very close to the ''transition temperature'' observed in DMTA thermograms whose data are in Table I. Correspondingly the crystallinity tends to diminish. Although the difference in T_{trans} is subtle (difference of 2°C), this is real as all the samples were conditioned in the same drying process; excluding the chance of moisture influence on T_{trans}. To study the effect of moisture on the glass transition temperature, a particular PU (PU-85) was subjected to DSC analysis after keeping the sample outside for 1 week. It was noticed that its T_{trans} decreased (by 5°C) because of the moisture absorption. The comparative DSC thermograms of PU-85 are shown in Figure 4. The moisture effect that we encounter here is quite different from the

TABLE I
Polyurethane Formulations and Properties

Sample	Ratio of moles of PTMO : BD : TDI	Hard segment content (wt %)	Inherent viscosity (DMF, 25°C, Conc: 2%) (dL/g)	T_{trans} (°C) (taken from DMTA)	T_{trans} (°C) (taken from DSC)
PU-33	1 : 3 : 4	33	0.34	70	73
PU-50	1 : 7 : 8	50	0.20	68	70
PU-72	1 : 19 : 20	72	0.16	46	50
PU-85	1 : 45 : 46	85	0.24	43	49

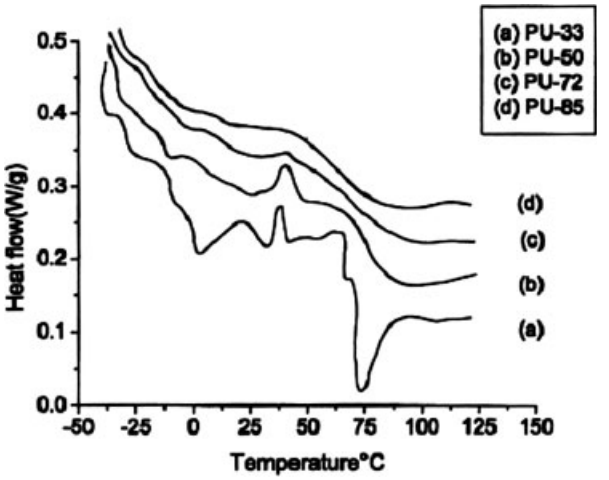

Figure 3 DSC thermograms of (a) PU-33, (b) PU-50, (c) PU-72, and (d) PU-85. Heating rate 5°C/min (first run).

moisture effect studies reported recently. Yang et al.[22] studied the effect of moisture on T_{trans} by immersion of PU samples in water for different hours. On the other hand, we studied the effects of moisture imbibed from the atmosphere. The influence of moisture is explained in detail in the IR study. It may be remarked that the analyzed samples were kept under dry conditions and exposed to moisture for minimum period during shape memory testing. Thus, the likely change in recovery characteristics due to change in T_{trans} as a result of moisture absorption can be considered as insignificant in the present case.

Spectroscopic analysis

FT-IR spectroscopic analyses were carried out to identify the urethane linkage and degree of phase separation (dps). Figure 5 shows the IR spectrum of PU-85. IR spectra showed the absence of —NCO

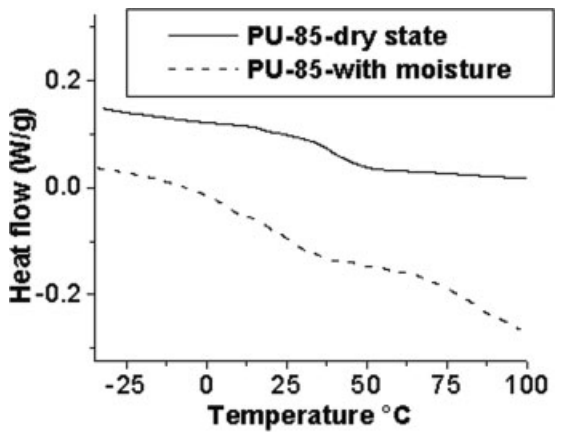

Figure 4 Comparative DSC thermograms of PU-85. Heating rate 5°C/min (first run).

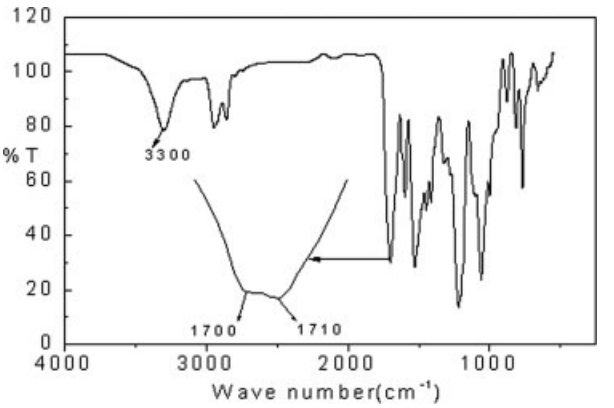

Figure 5 FTIR spectrum of PU-85 (thin film).

peak at 2200 cm^{-1} and —OH peak at 3500 cm^{-1} and the presence of urethane linkage. The characteristic absorption band of urethane C=O was split into two bands at 1710 and 1700 cm^{-1} because of the presence of intermolecular hydrogen bonding. Figure 6 shows the two nearer absorption bands of PU. These two-absorption peaks are due to the stretching vibration of carbonyl group in the hard segment of PU.[7,23] The peak at 1700 cm^{-1} is due to the presence of hydrogen-bonded carbonyl group. The intermolecular hydrogen bonding is between the carbonyl group and —NH— group in the hard segment leading to phase separation (which are not distinguishable in SEM). The degree of phase separation can thus be calculated from these two absorption bands at 1710 and 1700 cm^{-1} by using the following equation.

$$\text{dps} = P/(1+P) \tag{2}$$

where P is calculated as, $P = A_{1700}/A_{1710}$. A_{1708} and A_{1720} indicate the absorbances of the bands at 1710

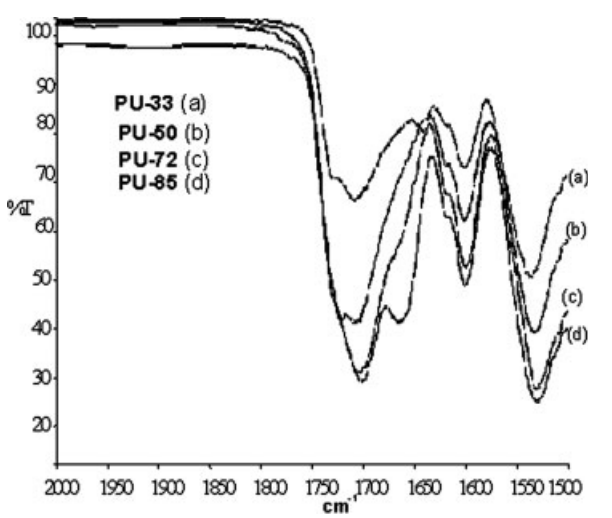

Figure 6 FTIR spectra (thin film) of carbonyl groups (a) PU-33, (b) PU-50, (c) PU-72, (d) PU-85.

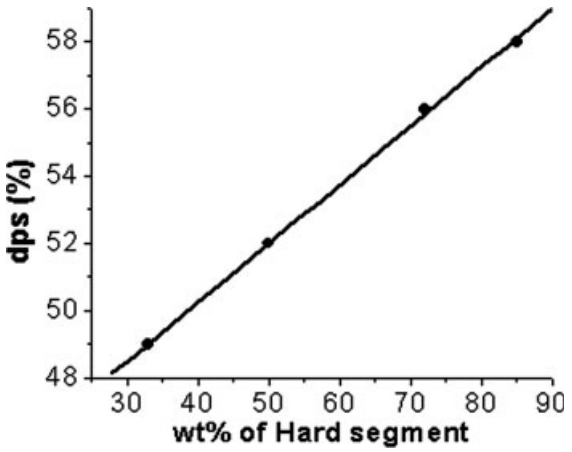

Figure 7 Dependency of degree of phase separation (dps) on hard segment.

and 1700 cm^{-1} respectively. *P* gives the ratio of these two peak absorbances. Figure 7 shows the dps vs. percentage of hard segments. As the hard segment content increases, the dps also increases proportionally, which implies the enhancement of interaction among hard segments through H-bonding. The degree of phase separation was also determined at varying temperatures, ie at room temperature, T_{trans}, (T_{trans} + 20°C) and at 100°C. Figure 8 shows the variation in dps with temperature for different polymer, showing that it is unaffected by temperature. These molecular interactions are responsible for the elastic strain recovery for the PU. To study the effect of absorbed moisture on the polymer characteristics, IR analysis was performed for a particular sample (PU-85) after keeping the sample outside for 1 week and also after heating the exposed sample at 100°C/1 h. Figure 9(a,b) show the comparative FTIR spectra of PU-85 under these conditions. Only a very minute

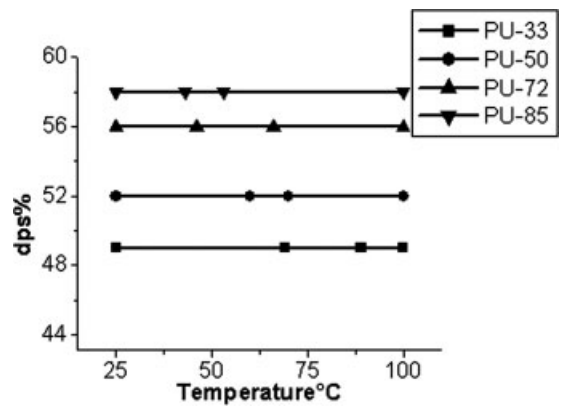

Figure 8 Dependency of phase separation (dps) on temperature for various Pus.

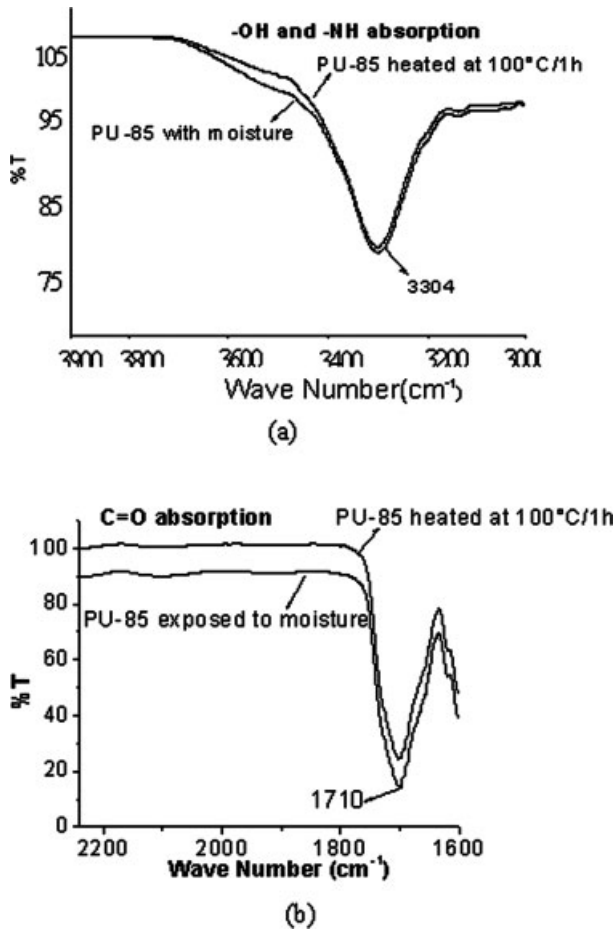

Figure 9 Comparative FTIR spectra of PU-85 (a) —OH and —NH absorption region, (b) C=O absorption region.

change occurred in –OH absorption (at 3500 cm^{-1}) because of the absorbed moisture. Yang et al.[22] reported that absorbed moisture could affect the C=O, —NH H—bonding (under their experimental conditions). In the sample handling conditions, we did not observe any such phenomena, as the —NH absorption at 3300 cm^{-1} and C=O at 1710 cm^{-1} remained intact before and after exposure to moisture (Fig. 9). Hence, it could be concluded that the effect of moisture is negligible in shape recovery characteristics in the present case.

X-ray diffraction studies

Figure 10 shows typical X-ray diffraction profiles obtained for the PUs. The diffraction profiles show an amorphous, diffused diffraction maximum at 2θ = 20°, suggesting the absence of defined PTMO crystallites. It is likely that some soft segment-hard segment phase mixing could occur in the system disturbing the soft segment crystallization.[4] This may account for the broader diffraction. PU-33 with maximum PTMO concentration showed a small diffrac-

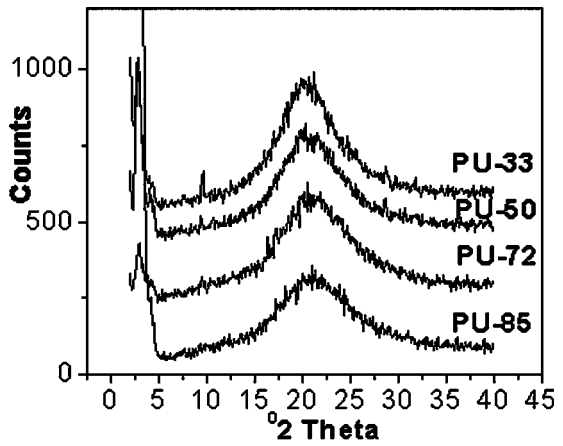

Figure 10 X-ray diffraction profiles of Pus.

tion peak at $2\theta = 9^\circ$, indicating a small proportion of residual-ordered structure. Because the XRD were performed at temperature quite near or above the crystal melting temperature of PU, the X-ray diffractions could not detect characteristic diffractions arising from crystallites of PTMO. The weak, sharp scattering observed is some cases are indicative of residual crystallites. We have reexamined the XRD of one typical PU (PU-50) at a temperature at 10–15°C (lower than the crystal melting temperature of the sample) by subjecting a 0°C cooled sample to immediate X-ray diffraction analysis. The XRD pattern of this sample (PU-50) is shown in Figure 11. It showed sharp diffraction peaks at $2\theta = 9^\circ$ and $2\theta = 28^\circ$, corresponding to the crystalline peaks of PTMO. Thus, the soft segment can be induced to crystallize on cooling. The absence of crystalline diffraction in samples analyzed at ambient temperature (Fig. 10) is a consequence of the melting of the crystallites at the analysis temperature. Table II shows the average crystallite size calculated from Scherrer equation for diffused scattering at $2\theta = 20^\circ$ for different polymer. In these cases, as the hard segment-content increases L_c decreases, confirming the broader crystal dispersion due to a decrease in the concentration of PTMO content. Notwithstanding the temperature effect, the excess hard segment content does not provide any ordered structure and probably disrupts the likely ordered structure of PTMO by way, possibly, of H-bonding interaction of NH with the PTMO groups as shown in Figure 12. The XRD pattern is generally in league with the DSC profiles, which showed sharp crystalline melting for PTMO rich systems and broad, diffuse transition for the PTMO starved PUs.

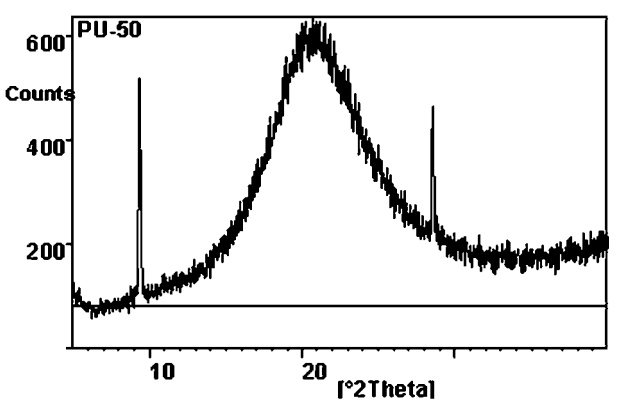

Figure 11 X-ray diffraction profile of cooled PU-50.

TABLE II
Variation of L_c with Hard Segment Content

Hard segment content (wt %)	L_c (Å)
33	41.6
50	35.6
72	29.7
85	27.7

SEM analysis

SEM analyses of typical PUs are shown in Figure 13. The SEM pictures correspond to the cross section of the polymers by exposing the surface of freshly broken samples. The micro phase domains of the hard segments are not differentiated in SEM. It showed some crystallites of the soft segment at higher PTMO content (PU-33). As the hard segment content increases, phase miscibilisation is seen (at the temperature range, 25°C of SEM). Thus DSC, XRD and SEM analysis are in agreement with one another as far as the phase morphology is concerned.

Mechanical properties

Ultimate tensile properties of PU copolymers with various hard segment contents are given in Table III. A typical stress-strain graph of PU-72 is shown in Figure 14. The behavior is typical of an elastomer. Tensile strength and percentage elongation decrease almost linearly with hard segment content. The elongation at break was the highest at 33 wt % of hard segment content, which was about 2–4 times that of the other samples. PUs with lower hard-segment

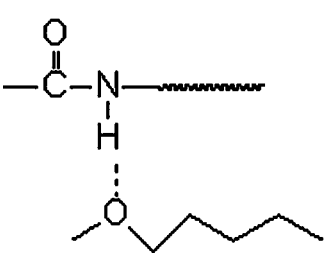

Figure 12 Possible H-bonding between urethane and PTMO.

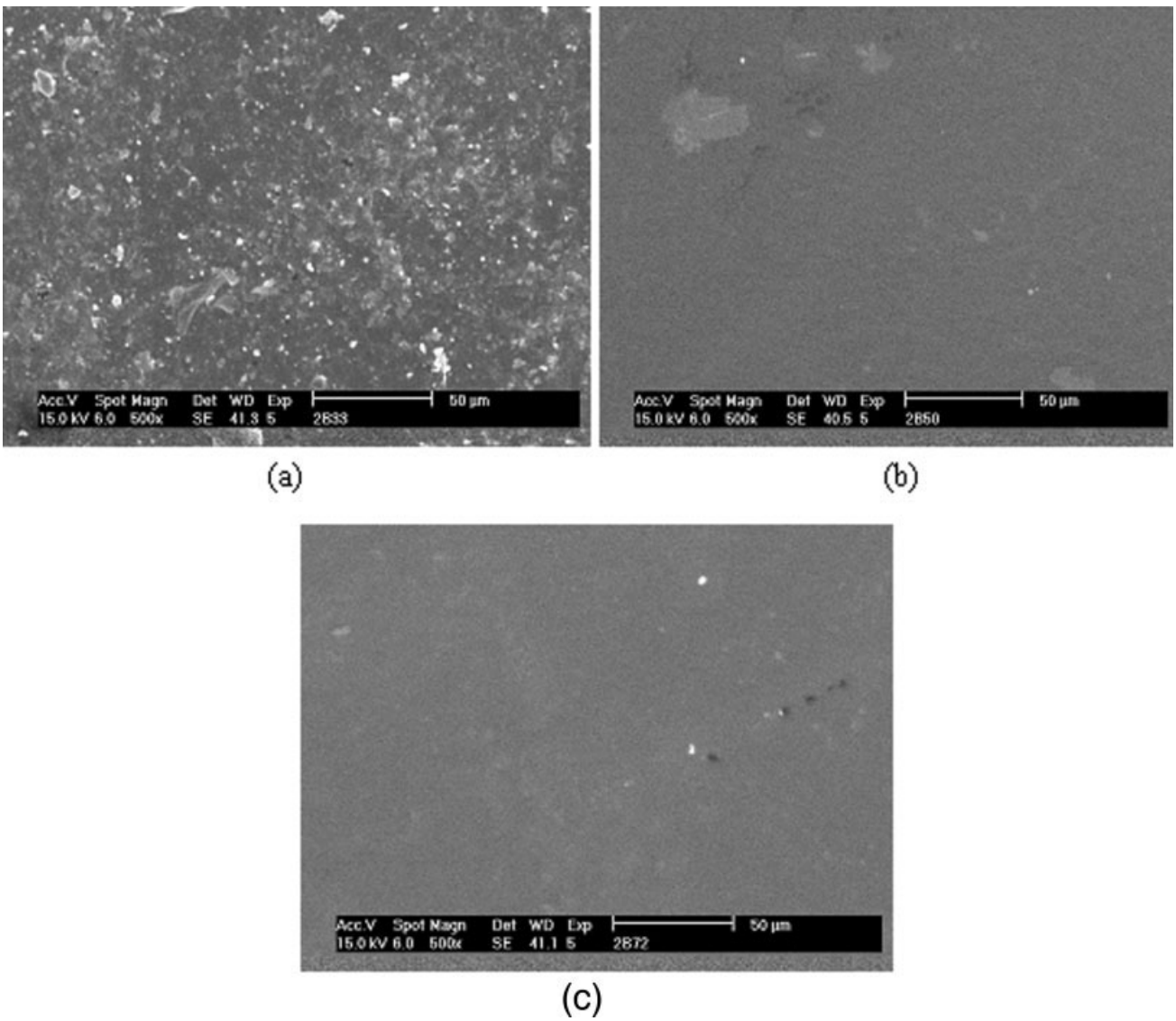

Figure 13 SEM analysis of (a) PU-33, (b) PU-50, (c) PU-72.

contents have a higher proportion of the comparatively high molecular weight PTMO unit, which imparts enhanced flexibility for the polymers resulting in the higher elongation. At high hard segment-content, the polymer becomes more rigid making it difficult to stretch, accounting for reduced elongation. This is reflected also in the initial modulus values for these systems. Thus, the mechanical properties of PU copolymers were found to be influenced by the ratio of soft/hard segment contents. An increase in molecular weight of PTMO would be expected to increase the tensile strength and elongation of the resulting polyurethanes by way of reducing the crosslink density and promoting the cohesive strength through dipolar interaction of the PTMO segments. If the crosslink density is maintained the same while enhancing the molecular weight of PTMO segment, this could lead to comparatively stronger polymer. However, this aspect was not examined in this work.

Dynamic mechanical thermal analysis

Figure 15(a–d) show the dynamic mechanical thermal spectra of PU samples. The curves show the variation of tensile storage modulus E′, loss modulus E″

TABLE III
Mechanical Properties of PUs

Hard segment (%)	Tensile strength (MPa)	Percentage elongation	Initial modulus (MPa)
33	17.3	1200	10.5
50	15.7	590	16.3
72	5.4	460	38.2
85	4.9	300	110.0

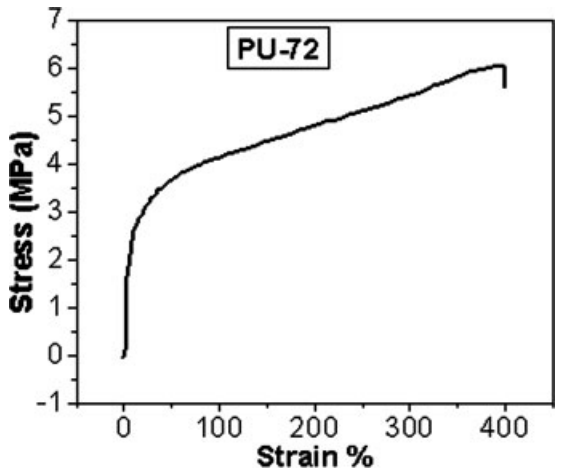

Figure 14 Stress-strain curve of PU-72.

and tan δ of the PUs with respect to temperature. All the PUs except PU-50 exhibit similar profiles of E′, E″, and tan δ. At high temperature, E′ increases in PU-50, which is apparently due to some chain extension reaction. The reanalyzed result of PU-50 is shown in Figure 15(b). Because the modulus increases at high temperature, PU-50 lacked shape memory property. Generally, large difference in modulus ratio is conducive to exhibiting fast shape recovery. For the rest of PUs, increasing hard segment content (that acts as a physical crosslinks) raised the glassy modulus. This implies a more rigid structure for the polymer containing higher proportion of BD and TDI units. The glassy modulus is due to the presence of elastic energy of both the PTMO phase and urethane phase. The rubbery modulus is due to the entropy elasticity of the two-phase structure of the material as reported.[4] It is seen that higher hard segment content leads to higher E_g and lower E_r, resulting in a large modulus ratio, which is conducive to a better shape recovery property. A large glassy state modulus leads to large shape fixity upon cooling and unloading.[4] Thus, PU-85 with large glassy state modulus has better shape fixity.

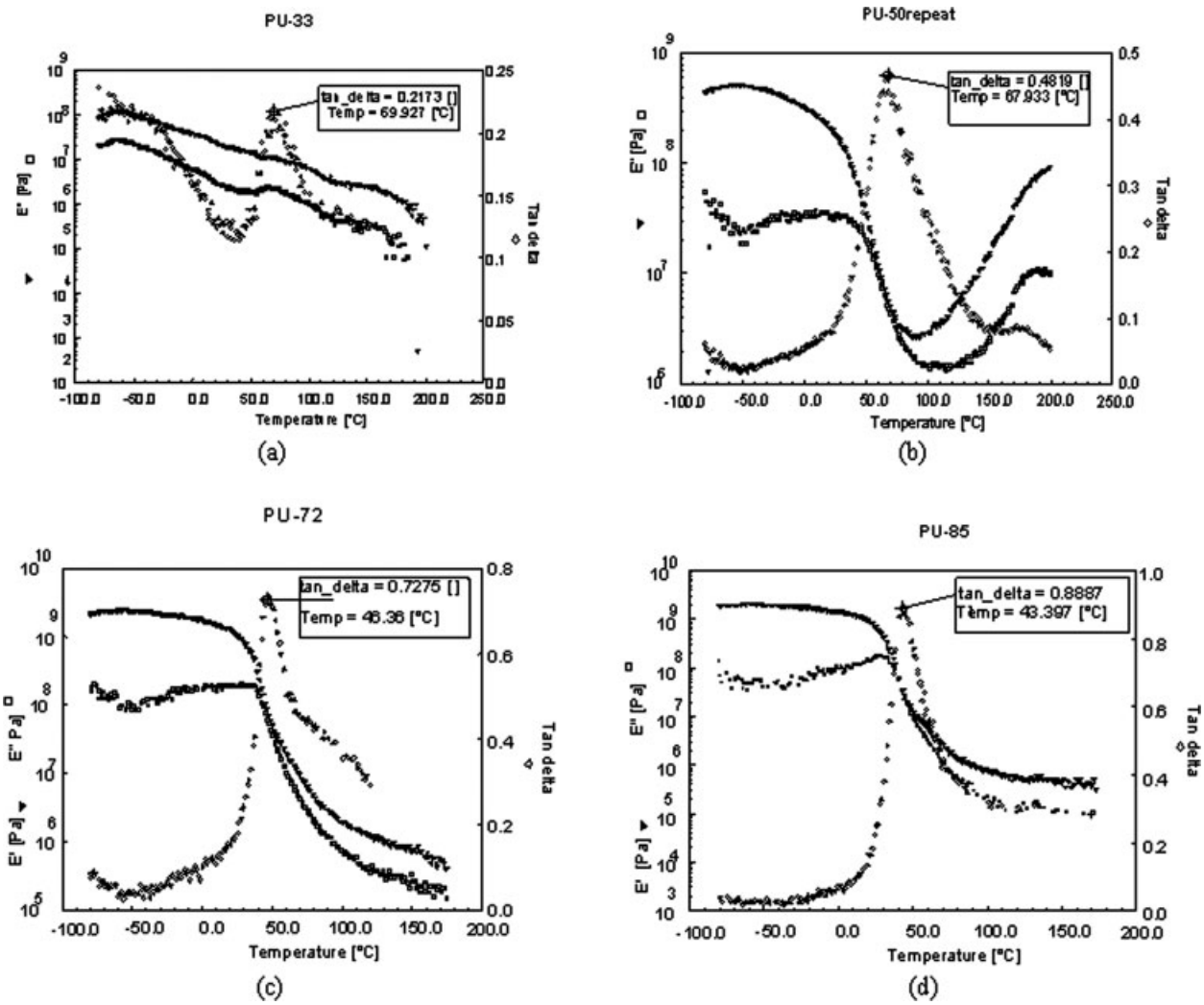

Figure 15 DMTA spectra of samples (a) PU-33, (b) PU-50, (c) PU-72, and (d) PU-85.

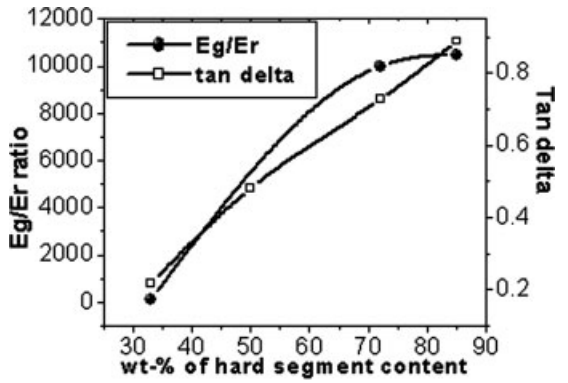

Figure 16 Variation of E_g/E_r ratio and tan δ with hard segment-content.

Figure 16 shows the variation of E_g/E_r ratio with hard segment-content. Comparing the ratio of E_g/E_r (modulus of glassy state / modulus of rubbery state), it is observed that there is a gradual increase in this parameter as the hard segment content gets enriched. Therefore, a better shape recovery property is expected from PU-85. Interestingly, the tan δ value increases with hard segment concentration. Higher loss tangent value indicates that the material tends to be more viscous. It is interesting to note that the tanδ is inversely related to the crystallisability of PU. Further, with increase in hard segment content, the tan δ value shifted to lower temperature. In all probability, the major transition observed at around 40–50°C is due to a combination of the melting of the PTMO crystallites and the glass transition of the amorphous segments. These trends are for PU containing varying concentration of PTMO of fixed molecular weight (2000). It can be expected that the trend will be different on enhancing the molecular weight of PTMO segments while keeping the hard segment content the same. In this case, the glassy modulus should increase, thanks to the better crystallization of PTMO segments leading to a better shape fixity and faster shape recovery.

Cyclic tensile behavior

Figure 17(a–d) show the typical cyclic stress-strain behavior of PU samples. Five thermo mechanical cycles were carried out in each case. As the number of cycles (N) increases, the slope of the loading

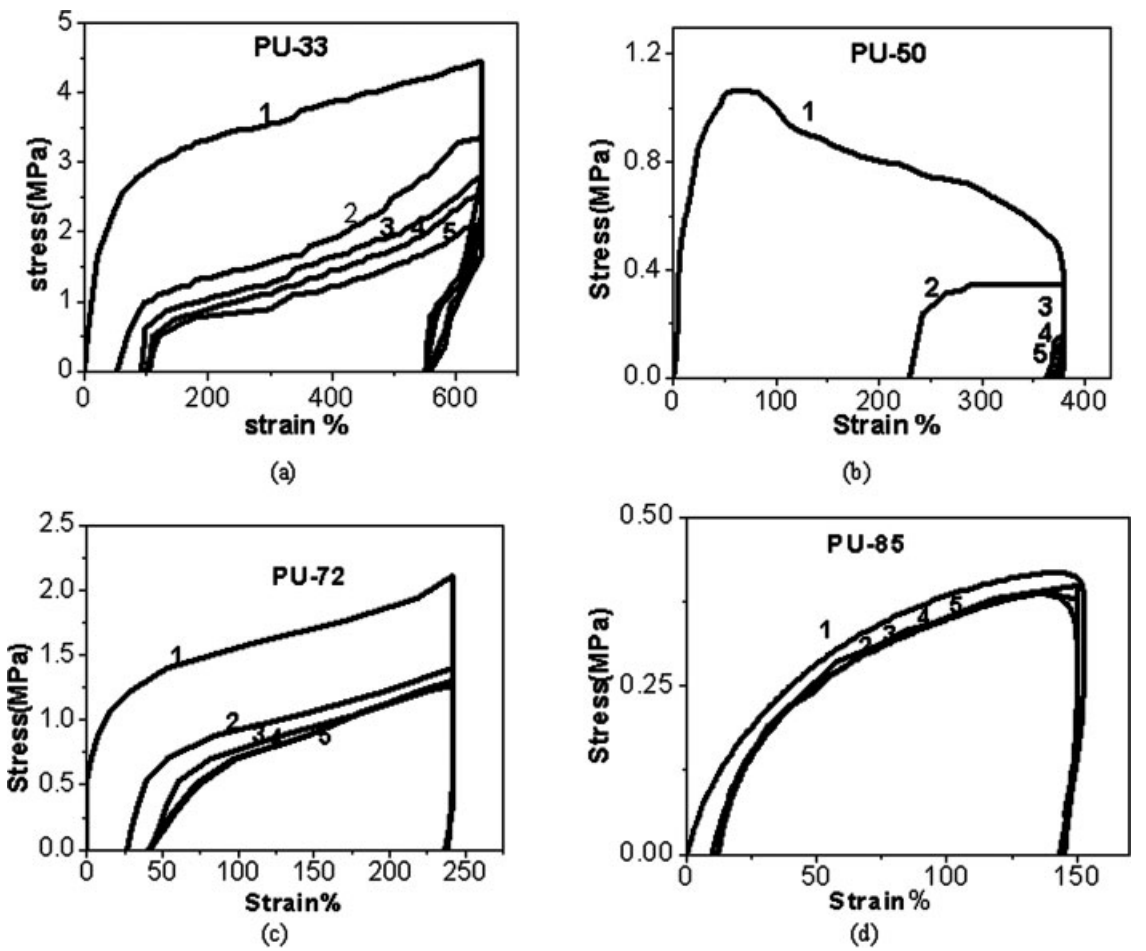

Figure 17 Cyclic tensile behavior of samples (a) PU-33, (b) PU-50, (c) PU-72, and (d) PU-85.

curve of PU-50 increases to a large extent than the rest of PUs. This is due to the increase in deformation resistance of the material with cycling.[17] This cyclic hardening can also be caused by the orientations of PU segments, thus, resulting in lack of shape memory property. It has been noted that the shape memory characteristics of the segmented PUs having crystallisable soft segments are closely related to the temperature dependent dynamic mechanical properties of the material.[4] PU-50 exhibited an unusual DMA behavior and lacked shape memory property. Incidentally, this system possessed minimum difference in modulus below and above the transition temperature (E_g/E_r). PU-50 exhibited this peculiar behavior even on repeated synthesis and analysis. The reason for its special behavior is not fully understood. The original shape is almost recovered for PU-85 due to the strong interactions among the hard segment components. When stress is applied to the PUs, soft segment will be preferentially extended in the stress direction rather than hard segment due to the fact that hard segment is close to glassy state and soft segment is rubbery above the transition temperature. The percentage shape recovery and shape fixity of the polymers were calculated as follows.

$$\text{Shape fixity} = (\varepsilon_u/\varepsilon_m) \times 100 \quad (3)$$

$$\text{Shape recovery} = (\varepsilon_r/\varepsilon_m) \times 100 \quad (4)$$

The shape fixity and shape recovery of PUs increase with increase in hard segment content. In fact, all the samples except PU-50 exhibited more than 82% shape fixity and shape recovery. Data in Table IV show the increasing trend of shape recovery and shape fixity of PUs with increase in hard segment-content. The highest shape fixity (97%) and shape recovery (92%) were observed for PU-85 with highest hard segment content. Thus, higher hard segment content is imperative for better shape memory property. This implies that moderate soft segment content in combination with good proportion of hard segment is conducive to imparting shape memory characteristics to the polyurethanes.

TABLE IV
Variation of Shape Recovery and Shape Fixity with Hard Segment-Content

% of hard segment content	% of shape recovery	% of shape fixity
33	83	85.8
72	84	96.6
85	92	97.3

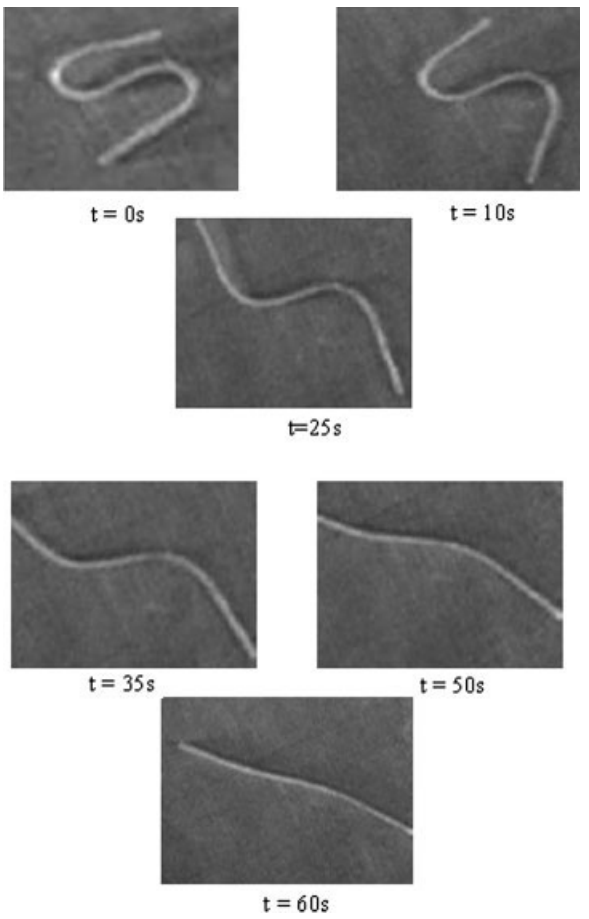

Figure 18 Shape recovery of PU-85 tape at different time interval at 75°C.

The shape recovery of PU-85 was experimentally demonstrated. The demonstration was done by processing a tape of 50 mm length, 10 mm breadth and 1 mm thickness. It was heated at 75°C (above T_{trans}) and distorted and frozen in an ice bath. The deformed sample retained the shape at ambient. When put in a hot bath at 70°C, the shape was recovered in about a minute. The different stages of shape recovery are demonstrated in Figure 18.

CONCLUSIONS

PUs based on PTMO, BD, and TDI were synthesized by varying the hard segment content between 33 and 85%. An increase in hard segment content resulted in diminution molecular weight, apparent T_{trans}, tensile strength and elongation of the PU. Modulus increased proportional to hard segment-content. FTIR spectroscopic gave evidence for increase in degree of phase segregation of urethane by way of H-bonding on augmenting the hard segment content. The XRD analysis showed PUs to be possessing both defined and diffused crystallinity at ambient temperatures. Crystallinity increased with

PTMO concentration and on lowering the temperature. SEM analysis showed the crystalline phase of soft segment in PTMO-rich composition. Storage modulus, E_g/E_r ratio as well as the shape recovery property showed an increasing trend with the hard segment content.

More than 85% shape recovery was achieved for system with hard segment content greater than 73%. Shape recovery as high as 96% was observed for system with maximum hard segment-content in the series. Extrapolation of the above results leads to the further conclusion that, increasing the molecular weight of PTMO segment (while keeping the other parameters same) would lead to a stronger PU with relatively higher transition temperature. The higher glassy modulus in this case is expected to increase the shape fixity and to diminish the recovery time. Decreasing the hard segment content can increase the mechanical properties and transition temperature, but is likely to adversely affect the shape memory properties.

Thus, by control of PU architecture with hard-soft segment combination, it is possible to realize SMP of desired recovery characteristics.

The authors acknowledge VSSC for granting permission to publish this article. Thanks are due to Mrs. Sadhana for the FTIR analyses and IICT, Hydrabad for DMTA spectra. Ms. J. D. Merline thanks University Grants Commission, New Delhi for a research fellowship.

References

1. Takahashi, T.; Hayashi, N.; Hayashi, S. J Appl Polym Sci 1996, 60, 1061.
2. Kim, B. K.; Lee, S.; Lee, Y.; Baek, S. Polymer 1998, 39, 2803.
3. Ken Gall; Dunn, M. L.; Liu, Y.; Finch, D.; Lake, M.; Munshi, N. A. Acta Mater 2002, 50, 5115.
4. Kim, B. K.; Lee, S. Y.; Xu, M. Polymer 1996, 37, 5781.
5. Jeong, H. M.; Lee, J. B.; Lee, S. Y.; Kim, B. K. J Mater Sci 2000, 35, 279.
6. Gouher, R.; Heinrich, L.; Arno, K. Polymer 2006, 47, 4251.
7. Cho, J. W.; Lee, S. H. Eur Polym J 2004, 40, 1343.
8. Li, F.; Richard, C. Larock. J Appl Polym Sci 2002, 84, 1533.
9. Lin, J. R.; Chen, L. W. J Appl Polym Sci 1999, 73, 1305.
10. Wang, M.; Zhang, L. J Polym Sci Part B: Polym Phys 1999, 37, 101.
11. Lin, J. R.; Chen, L. W. J Appl Polym Sci 1998, 69, 1575, 1563.
12. Lendlein, A.; Langer, R. Science 2002, 296, 1673.
13. Jeong, H. M.; Kim, B. K.; Ahn, B. K. Polym Int 2000, 49, 1714.
14. Zhu, G.; Liang, G.; Xu, Q.; Yu, Q. J Appl Polym Sci 2003, 90, 1589.
15. Lendlein, A.; Schmidt, A. M.; Schroeter, M.; Langer, R. J Polym Sci Part B: Polym Chem 2005, 43, 1369.
16. Changchun, M.; Wenjin, C.; Jianzhong, B.; Shenguo, W. Poly. Adv Technol 2005, 16, 608.
17. Tobushi, H.; Hayashi, S.; Kojima, S. JSME Int J 1992, 35, 296.
18. Lendlein, A.; Kelch, S. Angew Chem Int Ed Engl 2002, 41, 2034.
19. Kim, B. K.; Shin, Y. J.; Cho, S. M.; Jeong, H. M. J Polym Sci Part B: Polym Phys 2000, 38, 2652.
20. Shirai, Y.; Hayashi, S. Mitsubishi Tech Bull 1988, 184, 1.
21. Kobayashi, K.; Shunichi, H. U.S. Pat. 5,128,197 (1992).
22. Yang, B.; Huang, W. M.; Li, C.; Li, L. Polymer 2006, 47, 1348.
23. Lee, B. S.; Chun, B. C.; Chung, Y. C.; Sul, K.; Cho, J. W. Macromolecules 2001, 34, 6431.